



Oct 15th, 12:00 AM

Laterally Braced Cold-formed Steel Flexural Members with Edge Stiffened Flanges

Benjamin W. Schafer

Teoman Pekoz

Follow this and additional works at: <https://scholarsmine.mst.edu/isccss>



Part of the [Structural Engineering Commons](#)

Recommended Citation

Schafer, Benjamin W. and Pekoz, Teoman, "Laterally Braced Cold-formed Steel Flexural Members with Edge Stiffened Flanges" (1998). *International Specialty Conference on Cold-Formed Steel Structures*. 4. <https://scholarsmine.mst.edu/isccss/14iccfsss/14iccfsss-session1/4>

This Article - Conference proceedings is brought to you for free and open access by Scholars' Mine. It has been accepted for inclusion in International Specialty Conference on Cold-Formed Steel Structures by an authorized administrator of Scholars' Mine. This work is protected by U. S. Copyright Law. Unauthorized use including reproduction for redistribution requires the permission of the copyright holder. For more information, please contact scholarsmine@mst.edu.

LATERALLY BRACED COLD-FORMED STEEL FLEXURAL MEMBERS WITH EDGE STIFFENED FLANGES

By B.W. Schafer¹ & T. Peköz²

Abstract: The moment capacity of a laterally braced cold-formed steel flexural member with edge stiffened flanges (e.g., a channel or zee section) may be adversely affected by local or distortional buckling. Traditional design methods recognize the need to explicitly account for local buckling, but not distortional buckling. Experimental data and numerical analyses suggest that proper strength prediction of laterally braced cold-formed steel flexural members requires explicit treatment of distortional buckling. New procedures for hand prediction of the buckling stress in the local and distortional mode are presented. Numerical investigations are employed to highlight post-buckling behavior unique to the distortional mode. A new design method for flexural members is presented. The method integrates distortional buckling into the unified effective width approach currently used in most cold-formed steel design specifications. Comparison to experimental tests shows the viability and advantages of the new approach.

INTRODUCTION

Finite strip analysis of a flexural member with an edge stiffened flange (Figure 1) reveals three fundamental buckling modes: local, distortional, and lateral-torsional. For a laterally braced flexural member the lateral-torsional mode is restricted. Therefore, the two primary modes of concern are local and distortional.

The American Iron and Steel Institute Specification for the Design of Cold-Formed Steel Structural Members (AISI 1996), hereon referred to as the AISI Specification, attempts to account for distortional buckling through an empirical reduction of the local plate buckling coefficient, k . The empirical k values do not agree with the actual distortional buckling stress. The experimental work (Desmond et al. 1981) conducted to determine the reduced k , concentrated efforts on local buckling of the flange. Experimentally, this was accomplished by using back to back sections, such that the web did not buckle. This experimental setup strongly restricts distortional buckling. More recent experiments on laterally braced flexural members with edge stiffened flanges by Willis and Wallace (1990), Schuster (1992), Moreyra (1993), and Ellifritt (1997) demonstrate unconservative strength prediction using the AISI Specification.

A hand method for the prediction of the distortional buckling stress in compression members was derived by Lau and Hancock (1987). Hancock extended this approach to flexural members in Hancock (1995) and Hancock (1997). In Hancock et al.

1. Instructor, Cornell University, School of Civil and Environmental Engineering

2. Professor, Cornell University, School of Civil and Environmental Engineering

(1996) a method for evaluating the strength in distortional buckling is proposed. Hancock et al.'s method provides an independent strength calculation for distortional buckling. The suggested design strength is the minimum of the AISI Specification method and a distortional buckling method. Comparison of this approach to test data is favorable, though the method proves overly conservative in many cases.

A unified treatment of local and distortional buckling in laterally braced flexural members with edge stiffened flanges is sought here. The procedure begins with closed-form prediction of the local and distortional buckling stress. Interaction of the flange, web, and lip in both local and distortional buckling is considered. A need for the integration of the distortional mode into the design procedure is highlighted by two behavioral phenomena. First, the distortional mode has less post-buckling capacity than the local mode. Second, the distortional mode has the ability to control failure even when it occurs at a higher critical stress than the local mode. A design method incorporating these phenomena is needed to provide an integrated approach to strength prediction involving local and distortional buckling.

ELASTIC BUCKLING

The elastic buckling of cold-formed steel members may readily be predicted by numerical methods. However, for design procedures, closed-form solutions are still required. Therefore, new hand methods are developed for prediction of the buckling stress in the local and distortional modes.

LOCAL BUCKLING PREDICTION

An element model and a semi-empirical interaction model are presented for closed-form approximation of the buckling stress in the local mode (see Figure 1a). The element model ignores interaction of the flange, web, and/or lip. For instance, for a compression flange, it is assumed that the element is simply supported on all four sides and thus a plate buckling coefficient of $k = 4$ is employed. For the semi-empirical interaction model local buckling of the flange is influenced by its attachment to a lip and a web.

Expressions for the plate buckling coefficients for the element model and the semi-empirical interaction model are summarized in Table 1. All of the k values are written in terms of the critical buckling stress of the flange, where:

$$f_{cr} = k \frac{\pi^2 D}{b^2 t} \quad (1)$$

Several of the elements are subjected to a stress gradient, which is defined in terms of ξ ,

$$\xi = \frac{f_1 - f_2}{f_1} \quad (2)$$

Where, f_1 and f_2 are defined as the stresses at the opposite edges of the element. For the web, f_1 is at the web/compression flange juncture. For the lip, f_1 is at the lip/compression flange juncture. Compression stresses are positive.

With the exception of the $k = 4$ solution, all of the expressions in Table 1 are new. The equations in Table 1 are determined by fitting expressions to finite strip analysis

results. Figure 2 shows the comparison for the local buckling expressions of an isolated flange and lip. The element model provides a lower bound, while the semi-empirical interaction model closely approximates the finite strip analysis, within prescribed parameters.

DISTORTIONAL BUCKLING PREDICTION

Prediction of distortional buckling, as shown in Figure 1b, is complicated due to the sensitivity of the solution to the rotational restraint at the web/compression flange juncture. Consider an isolated flange and lip (similar to the inset of Figure 2) in which the web/flange juncture is idealized as either a simple support or a fixed support. Finite strip analysis (Figure 3) shows that for local buckling the change in the plate buckling coefficient is small regardless of the boundary condition. However, for distortional buckling the potential differences are significant.

Closed-form prediction of the distortional buckling stress is based on an examination of the rotational restraint at the web/flange juncture. Consider a typical cross-section as shown in Figure 4 and the definition of the rotational stiffness. The rotational stiffness may be expanded as a summation of elastic and stress dependent geometric stiffness terms with contributions from both the flange and the web,

$$k_{\phi} = \left(k_{\phi f} + k_{\phi w} \right)_e - \left(k_{\phi f} + k_{\phi w} \right)_g. \quad (3)$$

Buckling ensues when the elastic stiffness at the web/flange juncture is eroded by the geometric stiffness, i.e.,

$$k_{\phi} = 0. \quad (4)$$

Using (4) and writing the stress dependent portion of the geometric stiffness explicitly,

$$k_{\phi} = k_{\phi f e} + k_{\phi w e} - f \left(\tilde{k}_{\phi f g} + \tilde{k}_{\phi w g} \right) = 0. \quad (5)$$

Therefore, the buckling stress (f) is

$$f = \frac{k_{\phi f e} + k_{\phi w e}}{\tilde{k}_{\phi f g} + \tilde{k}_{\phi w g}}. \quad (6)$$

Analytical models are needed for determining the rotational stiffness contributions from the flange and the web. For the flange, cross-section distortion is not important (see Figure 1b). The flange is thus modeled as a column undergoing flexural-torsional buckling. This is similar to the approach of Sharp (1966), Lau (1988), Seah and Rhodes (1993), Hancock (1997), and Davies and Jiang (1996). For the web, cross-section distortion must be considered. The web is modeled as a single finite strip. Therefore, the transverse shape function is a cubic polynomial. The longitudinal shape functions of the flange and web are matched by using a single half sine wave for each.

Distortional Buckling – Model for the flange

Consider the flexural-torsional buckling of a column with springs along one edge as shown in Figure 5. The governing differential equations are:

$$EI_{yf} \frac{d^4 u}{dz^4} + EI_{xyf} \frac{d^4 v}{dz^4} + P \left(\frac{d^2 u}{dz^2} + y_o \frac{d^2 \phi}{dz^2} \right) + k_{xf} \left(u + (y_o - h_y) \phi \right) = 0, \quad (7)$$

$$EI_{xf} \frac{d^4 v}{dz^4} + EI_{xyf} \frac{d^4 u}{dz^4} + P \left(\frac{d^2 v}{dz^2} - x_o \frac{d^2 \phi}{dz^2} \right) + k_{yf} \left(v - (x_o - h_x) \phi \right) = 0, \quad (8)$$

$$EC_{wf} \frac{d^4 \phi}{dz^4} - \left(GJ_f - \frac{I_{of}}{A_f} P \right) \frac{d^2 \phi}{dz^2} - P \left(x_o \frac{d^2 v}{dz^2} - y_o \frac{d^2 u}{dz^2} \right) + k_{xf} \left(u + (y_o - h_y) \phi \right) (y_o - h_y) - k_{yf} \left(v - (x_o - h_x) \phi \right) (x_o - h_x) + k_{\phi} \phi = 0. \quad (9)$$

Where I_{xf} , I_{yf} , I_{xyf} , I_{of} , C_{wf} , J_f and A_f are section properties of the flange, k_{xf} , k_{yf} , and k_{ϕ} are the springs, x_o and y_o are the distances from the centroid to the shear center, and h_x and h_y are the distances from the centroid to the springs. The following shape functions consistent with a simply supported column are used:

$$\phi = A_1 \sin\left(\frac{\pi z}{L}\right), \quad u = A_2 \sin\left(\frac{\pi z}{L}\right), \quad v = (x_o - h_x) A_1 \sin\left(\frac{\pi z}{L}\right) \quad (10)$$

For this application the k_{xf} spring is assumed zero and the k_{yf} spring is assumed infinite. The typical approach is to find the buckling load, P_{cr} . However, the goal here is to write the solution in terms of the rotational restraint the flange provides to the web/flange juncture. The shape functions (11) - (12) are substituted into (7) - (9) and the load, P , is written in terms of the uniform stress, f_1 . If terms of order f^2 are neglected then the flange rotational restraint may be written in the linear form given in (5). The resulting rotational stiffness terms are

$$k_{\phi e} = \left(\frac{\pi}{L} \right)^4 \left(EI_{xf} (x_o - h_x)^2 + EC_{wf} - E \frac{I_{xyf}^2}{I_{yf}} (x_o - h_x)^2 \right) + \left(\frac{\pi}{L} \right)^2 GJ_f, \quad (11)$$

$$\tilde{k}_{\phi s} = \left(\frac{\pi}{L} \right)^2 \left[A_f \left((x_o - h_x)^2 \left(\frac{I_{xyf}}{I_{yf}} \right)^2 - 2y_o (x_o - h_x) \left(\frac{I_{xyf}}{I_{yf}} \right) + h_x^2 + y_o^2 \right) + I_{xf} + I_{yf} \right]. \quad (12)$$

For a simple lip stiffened flange (Figure 5) the section properties in (11) and (12) are only a function of b , d , θ , and t :

$$A_f = (b + d)t, \quad (13)$$

$$J_f = \frac{1}{3}bt^3 + \frac{1}{3}dt^3, \quad (14)$$

$$I_{xf} = \frac{t(t^2b^2 + 4bd^3 - 4bd^3 \cos^2(\theta) + t^2bd + d^4 - d^4 \cos^2(\theta))}{12(b + d)}, \quad (15)$$

$$I_{yf} = \frac{t(b^4 + 4db^3 + 6d^2b^2 \cos(\theta) + 4d^3b \cos^2(\theta) + d^4 \cos^2(\theta))}{12(b+d)}, \quad (16)$$

$$I_{xyf} = \frac{tb d^2 \sin(\theta)(b+d \cos(\theta))}{4(b+d)}, \quad (17)$$

$$I_{of} = \frac{tb^3}{3} + \frac{bt^3}{12} + \frac{td^3}{3}, \quad (18)$$

$$x_o = \frac{b^2 - d^2 \cos(\theta)}{2(b+d)}, \quad (19)$$

$$h_y = y_o = \frac{-d^2 \sin(\theta)}{2(b+d)}, \quad (20)$$

$$h_x = \frac{-(b^2 + 2db + d^2 \cos(\theta))}{2(b+d)}, \quad (21)$$

$$x_o - h_x = b, \quad (22)$$

$$C_{wyf} = 0. \quad (23)$$

Distortional Buckling – Model for the Web

Derivation of the rotational restraint provided by the web to the web/flange juncture is based on using a single finite strip as shown in Figure 6. The finite strip solution for the plate bending terms may be symbolically represented as:

$$\begin{Bmatrix} \underline{F}_1 \\ \underline{M}_1 \\ \underline{F}_2 \\ \underline{M}_2 \end{Bmatrix} = \begin{bmatrix} k_{11} & k_{12} & k_{13} & k_{14} \\ k_{21} & k_{22} & k_{23} & k_{24} \\ k_{31} & k_{32} & k_{33} & k_{34} \\ k_{41} & k_{42} & k_{43} & k_{44} \end{bmatrix}_E - \begin{bmatrix} k_{11} & k_{12} & k_{13} & k_{14} \\ k_{21} & k_{22} & k_{23} & k_{24} \\ k_{31} & k_{32} & k_{33} & k_{34} \\ k_{41} & k_{42} & k_{43} & k_{44} \end{bmatrix}_G \begin{Bmatrix} w_1 \\ \theta_1 \\ w_2 \\ \theta_2 \end{Bmatrix} \quad (24)$$

Where \underline{F} and \underline{M} refer to consistent nodal loads or moments and the k_{ij} terms are stiffness coefficients for the plate bending finite strip matrix, (e.g. Cheung 1976). For simply supported edges, the terms of interest are:

$$\begin{Bmatrix} \underline{M}_1 \\ \underline{M}_2 \end{Bmatrix} = \begin{bmatrix} k_{22} & k_{24} \\ k_{42} & k_{44} \end{bmatrix}_E - \begin{bmatrix} k_{22} & k_{24} \\ k_{42} & k_{44} \end{bmatrix}_G \begin{Bmatrix} \theta_1 \\ \theta_2 \end{Bmatrix} \quad (25)$$

In order to find $k_{\phi w}$ consider the strip to be unloaded along edge 2 and loaded along edge 1 (the web/compression flange juncture) with a sinusoidal edge moment of $M \sin(\pi y/L)$. The consistent nodal moments $\underline{M}_2 = 0$, and $\underline{M}_1 = \frac{1}{2}ML$ are substituted. The solution is then written in terms of θ_1 . If $\theta_1 = 1$, then $M = k_{\phi w}$, therefore:

$$k_{\phi w} = \frac{2}{L} \left((k_{22e} - k_{22g}) - \frac{(k_{24e} - k_{24g})(k_{42e} - k_{42g})}{(k_{44e} - k_{44g})} \right) \quad (26)$$

The web rotational stiffness, $k_{\phi w}$, is decomposed into elastic and geometric parts:

$$k_{\phi w} = k_{\phi we} - k_{\phi wg}, \quad (27)$$

$$k_{\phi we} = \frac{2}{L} \left(k_{22e} - \frac{k_{24e}^2}{k_{22e}} \right), \quad (28)$$

$$-k_{\phi wg} = \frac{2}{L} \left(\left[(k_{22e} - k_{22g}) - \frac{(k_{24e} - k_{24g})(k_{42e} - k_{42g})}{(k_{44e} - k_{44g})} \right] - \left(k_{22e} - \frac{k_{24e}^2}{k_{22e}} \right) \right). \quad (29)$$

The k_{ij} terms may be substituted directly to yield the complete analytical expressions for k_{ϕ} . Although exact, the expressions have an inordinate number of terms. Simplifications are made in order to provide a more compact solution. The elastic rotational stiffness (28) is truncated by converting to partial fractions on the length, L , and keeping the constant term, the $1/L^2$ term, and the $1/L^4$ term. The resulting expression asymptotes to the full expression and provides a reasonable approximation of the elastic rotational stiffness,

$$k_{\phi we} = D \left(\frac{3}{h} + \left(\frac{\pi}{L} \right)^2 \frac{19h}{60} + \left(\frac{\pi}{L} \right)^4 \frac{h^3}{240} \right). \quad (30)$$

For the geometric rotational stiffness (29) the first approximation made is to linearize on the stress f_1 . This is adequate for stress gradients near pure bending ($\xi_{web} \sim 2$), but breaks down as the stress approaches pure compression ($\xi_{web} = 0$). With this simplification the geometric rotational stiffness takes the form:

$$-k_{\phi wg} = \frac{2f_1}{L} \left(\frac{2k_{22e}k_{24e}k_{24g} - k_{22g}k_{24e}^2 - k_{22g}k_{22e}^2}{k_{22e}^2} \right). \quad (21)$$

Further simplification is provided after substituting in the k_{ij} terms by converting the solution to partial fractions on the length, L . The general expression is then in 3 terms in which the denominators are

$$\frac{-}{L^2} + \frac{-}{(h^4 + L^2h^2 + L^4)} + \frac{-}{(h^4 + L^2h^2 + L^4)^2} \quad (32)$$

Parametric analysis shows the final term to be insignificant, thus it is neglected. The first two terms are combined to form the approximation of the rotational geometric stiffness, where:

$$k_{\phi w} = k_{\phi we} - f_1 \tilde{k}_{\phi wg}, \quad (33)$$

$$\tilde{k}_{\phi_{wg}} = \frac{ht\pi^2}{13440} \left(\frac{(45360(1 - \xi_{web}) + 62160) \left(\frac{L}{h}\right)^2 + 448\pi^2 + \left(\frac{h}{L}\right)^2 (53 + 3(1 - \xi_{web}))\pi^4}{\pi^4 + 28\pi^2 \left(\frac{L}{h}\right)^2 + 420 \left(\frac{L}{h}\right)^4} \right). \quad (34)$$

Distortional Buckling – Critical Length

The buckling stress is a function of length, L . To approximate the L at which f is a minimum, the rotational stiffness terms are rewritten explicitly in terms of L :

$$k_{\phi_{fe}} = (1/L)^4 C_1 + (1/L)^2 C_2, \quad (35)$$

$$\tilde{k}_{\phi_{fg}} = (1/L)^2 C_3, \quad (36)$$

$$k_{\phi_{ve}} = K_1 + (1/L)^2 K_2 + (1/L)^4 K_3, \quad (37)$$

$$\tilde{k}_{\phi_{vg}} = K_4(f(L)). \quad (38)$$

This gives the solution for the distortional buckling stress f as;

$$f = \frac{(1/L)^4 C_1 + (1/L)^2 C_2 + K_1 + (1/L)^2 K_2 + (1/L)^4 K_3}{(1/L)^2 C_3 + K_4(f(L))}. \quad (39)$$

The critical length is found by minimizing f with respect to L . This minimization is complicated by the K_4 term – the web geometric stiffness. If the $f(L)$ in the K_4 term is approximated as $1/L^2$ then the C_3 and K_4 terms drop out. This assumption is made, therefore, the general solution for L_{cr} is:

$$\frac{df}{dL} = 0 \rightarrow L_{cr} = \left(\frac{C_1 + K_3}{K_1} \right)^{1/4}. \quad (40)$$

The appropriate terms for C_1 , K_3 and K_1 are substituted, resulting in

$$L_{cr} = \left(\frac{4\pi^4 h(1 - \nu^2)}{t^3} \left(I_x (x_o - h_x)^2 + C_w - \frac{I_{xy}^2}{I_y} (x_o - h_x)^2 \right) + \frac{\pi^4 h^4}{720} \right)^{1/4}. \quad (41)$$

If the flange is assumed to be pinned (as is done in the critical length derivation of Lau 1988) then the $(I_{xy})^2/I_y$ term is assumed negligible.

Elastic Distortional Buckling – Summarized

To find the critical buckling stress in the distortional mode $(f_{cr})_{dist}$, use (6). The rotational stiffness terms in (6) are found in (11), (12), (30), and (34). The rotational stiffness terms should be evaluated at L_{cr} via (41) unless $L_b < L_{cr}$.

COMPARISON OF ELASTIC BUCKLING METHODS

Thirty-two members are examined via finite strip analysis to compare to the proposed hand methods. The critical local buckling moment (M_{local}) and critical distortional buckling moment ($M_{dist.}$) are recovered from the finite strip analysis. The geometry of the studied members is summarized in Table 2. The comparison of the predictions is in Table 3.

The models proposed for the local buckling stress (Table 1) do not directly provide a direct prediction of the critical buckling moment. For the element model the governing local buckling stress is assumed to be the minimum of the flange, web, or lip. For the interaction model the governing local buckling stress is assumed to be the minimum of the flange/lip and flange/web calculation. The governing local buckling stress is then used to determine the local buckling moment.

For local buckling prediction the interaction model performs markedly better than the element model. The overly conservative nature of the element model is largely driven by poor predictions when the lip controls the local buckling stress. In cases when the lip controls, the average $M_{predicted}/M_{local}$ ratio is 0.6. The proposed distortional buckling method compares favorably with finite strip analysis. Predictions for the $\theta = 45^\circ$ members are slightly less conservative than for the $\theta = 90^\circ$ members. Fortunately, the ratio for the $\theta = 45^\circ$ degree members is still 0.98 and the standard deviation is lower than for the $\theta = 90^\circ$ members.

POST-BUCKLING BEHAVIOR OF EDGE STIFFENED ELEMENTS

To investigate the post-buckling behavior in the local and distortional modes, nonlinear FEM analysis of isolated flanges is completed using ABAQUS (HKS 1995). The boundary conditions and the elements used to model the flange are shown in Figure 7. The material model is elastic-plastic with strain hardening. Initial imperfections in the local and distortional mode are superposed to form the initial imperfect geometry. A longitudinal through thickness flexural residual stress of $30\% f_y$ is also modeled.

The geometry of the members investigated is summarized in Table 4. The thickness is 1mm and $f_y = 345\text{MPa}$. The two basic failure mechanisms from the FEM analysis are shown in Figure 8. It is observed that the final failure mechanism is consistent with the distortional mode even in cases when the distortional buckling stress is higher than the local buckling stress. Consider Figure 9, which shows the final failure mechanism for all the members studied. Based solely on elastic buckling one would expect the local mode to control in all cases in which $(f_{cr})_{local} / (f_{cr})_{dist.} < 1$ – as the figure shows, this is not the case.

Finite element analysis also reveals that the post-buckling capacity in the distortional mode is less than that in the local mode. Consider Figure 10, for the same slenderness values the distortional failures exhibit a lower ultimate strength. Similar loss in strength is experimentally observed and summarized in Hancock et al. (1994).

The geometric imperfections are modeled as a superposition of the local and distortional mode. The magnitude of the imperfection is selected based on the statistical summary provided in Schafer and Peköz (1998). The error bars in Figure 10 demonstrate the range of strengths predicted for imperfections varying over the central 50% portion of

expected imperfection magnitudes. The greater the error bars, the greater the imperfection sensitivity.

The percent difference in the strength over the central 50% portion of expected imperfection magnitudes is used as a measure of imperfection sensitivity:

$$\frac{(f_u)_{25\% \text{ imp.}} - (f_u)_{75\% \text{ imp.}}}{\frac{1}{2} \left((f_u)_{25\% \text{ imp.}} + (f_u)_{75\% \text{ imp.}} \right)} \times 100\% . \quad (42)$$

A contour plot of this imperfection sensitivity statistic (42) is shown in Figure 11. Stocky members prone to failure in the distortional mode have the greatest sensitivity. In general, distortional failures are more sensitive to initial imperfections than local failures. Areas of imperfection sensitivity risk are assigned.

DESIGN OF FLEXURAL MEMBERS

The current AISI Specification approach for the capacity of a laterally braced flexural member involves determining an effective section modulus to account for local buckling. As shown in Figure 12, each element is reduced from its gross width (e.g., b) to an effective width (e.g., b_e). The reduction is based on an empirical correction to the work of von Kármán et al. (1932) completed by Winter (1947). The extension of this approach to all members of the cross-section is based on the unified approach of Peköz (1987). Once the effective width is calculated determination of the flexural strength becomes a relatively straightforward manner, as shown in Table 5.

Design – Effective Width of Elements

The effective width of the flange (or lip, replace b with d) is,

$$b_e = \rho b. \quad (43)$$

Where ρ is defined as

$$\rho = (1 - 0.22/\lambda)/\lambda \text{ for } \lambda > 0.673 \text{ otherwise } \rho = 1. \quad (44)$$

The slenderness parameter, λ , is

$$\lambda = \sqrt{f_y / (f_{cr})_{\text{flange}}} . \quad (45)$$

Portioning of the effective width for the flange is straightforward (see Figure 12). However, in the case of a stiffened element under a stress gradient (i.e., the web), the portioning of h to h_1 , h_2 , and h_t is not as straightforward. The expressions currently used in the AISI Specification for a stiffened element under a stress gradient are discontinuous (Cohen 1987) and unconservative (Figure 13). Other specifications, such as the Canadian Code for Cold-Formed Steel Structural Members (Canadian Standards Association 1991) yield results more consistent with numerical analysis.

A new approach is proposed for the effective width of stiffened elements under a stress gradient (i.e., webs). Consider the effective width of an element in pure compression as shown in Figure 14. Determination of the effective width is based on (1) an approximation of the nonlinear post-buckling stress via ρ and (2) a force balance between the approximated nonlinear stress and the effective section. For an element under

a stress gradient (Figure 14) the natural extension to this methodology is to determine the effective width by insuring that both a force and a moment balance are maintained between the approximated nonlinear stress and the effective section. The solution of this force and moment balance result in the following expressions:

$$h_1 = h\omega/\xi_{web} \quad (\text{for } \xi_{web} > 0), \quad (46)$$

$$h_2 = (h/\xi_{web})\sqrt{\omega^2 - 2\omega + \rho} \quad (\text{for } \xi_{web} > 0), \quad (47)$$

$$\lambda = \sqrt{f_y/(f_{cr})_{web}}, \quad (48)$$

$$\rho = (1 - 0.22/\lambda)/\lambda, \text{ for } \lambda > 0.673, \text{ else } \rho = 1, \quad (49)$$

$$\begin{aligned} 0 \leq \rho < 0.77 & \quad \omega = 0.33\rho \\ 0.77 \leq \rho < 0.95 & \quad \omega = 0.23 \\ 0.95 \leq \rho \leq 1.00 & \quad \omega = -4.6\rho + 4.6 \end{aligned} \quad (50)$$

The resulting expressions agree with numerical analysis (see Figure 13). Further, the effective width of the web is a function of ρ . Thus, for the first time, the effective width of an element under a stress gradient is a function of the degree of nonlinearity in the post-buckling stress distribution, as reflected through ρ .

Design – Integrating Distortional Buckling into the Procedure

If distortional buckling is considered then the critical buckling stress of an element (flange, web or lip) is no longer solely dependent on local buckling. In order to properly integrate distortional buckling, reduced post-buckling capacity in the distortional mode and the ability of the distortional mode to control the failure mechanism even when at a higher buckling stress than the local mode must be incorporated. Consider defining the critical buckling stress of the element used in (45) or (48) as:

$$(f_{cr}) = \min[(f_{cr})_{local}, R_d(f_{cr})_{dist.}] \quad (51)$$

For strength, if the reduced distortional mode governs, then (44) or (49) become:

$$\rho = \sqrt{R_d} \lambda (1 - 0.22\sqrt{R_d} \lambda) \quad (52)$$

For $R_d < 1$ this method provides an additional reduction on the post-buckling capacity. Further, the method also allows the distortional mode to control in situations when the distortional buckling stress is greater than the local buckling stress. Thus, R_d provides a framework for solving the problem of predicting the failure mode and reducing the post-buckling capacity in the distortional mode. The selected form for R_d based on Figure 9, Figure 10 and the experimental results of Hancock et al. (1994) is

$$R_d = \min\left(1, \frac{1.17}{\lambda_d + 1}\right) \text{ where } \lambda_d = \sqrt{f_y/(f_{cr})_{dist.}} \quad (53)$$

Two models are advanced for predicting the critical buckling stress of the elements. The models are summarized in Table 6. With f_{cr} of the element known the effective width of each element may readily be determined. The procedure outlined in Figure 12 and Table 5 is completed to calculate the section capacity.

Comparison to Experimental Data

Experimental tests on laterally braced flexural members with edge stiffened flanges from Cohen (1987), Desmond (1978), Elhouar and Murray (1985), Ellifritt et al. (1992), Ellifritt et al. (1997), LaBoube and Yu (1978), Moreyra (1993), Rogers (1995), Schardt and Schrade (1982), Schuster (1992), Shan et al. (1994), Willis and Wallace (1990) and Winter (1947) is gathered and examined. Based on the information available from the tests, the type of sections tested, and the loading arrangement, the applicability for use in this comparison is assessed. The experimental data of Desmond (1978), Ellifritt et al. (1992), Elhouar and Murray (1985), and Winter (1947) are deemed to have poor applicability. Desmond's and Winter's tests use back to back webs which provide an unrealistic rotational restraint. Ellifritt et al.'s (1992) tests primarily fail in the lateral-torsional mode. Elhouar and Murray's (1985) summary of proprietary tests does not provide enough detailed information on loading and bracing.

The majority of the remaining tests are on face to face channels in two-point bending. The channels typically have significant bracing at the load application point as well as a regularly spaced angle or bar attached across the two channels in both the compression flange and tension flange. The bracing is to insure lateral-torsional buckling does not occur, and to approximate the effect of sheeting. The small spacing of the attached angles, or bars (often 300mm ~12" or 150mm ~ 6") partially restricts the distortional mode.

If the bracing length (L_b) is less than the predicted L_{cr} from (41) then L_b is used in determining the distortional buckling stress. In many tests $L_b < L_{cr}$. Therefore capacity lower than the experimentally observed strength is possible even for a laterally braced member, due to the fact that the distortional mode is partially restricted.

The flexural capacity of the remaining test data is assessed via the AISI Specification (M_{AISI}) and the two proposed methods: M_1 and M_2 (see Table 6). The statistical results are summarized in Table 7. One striking feature that Table 7 does not bring out is the systematic error that exists in the current AISI Specification method for large h/b (see Figure 15).

From Table 7, the overall performance of the AISI Specification method appears adequate. A more detailed analysis reveals several inadequacies. For one, several of the individual tests groups yield consistently unconservative predictions ($n < 1$). Second, the systematic error for large h/b is problematic. Third, the AISI method is not a function of bracing length. Therefore, the same members at longer unbraced lengths (but members still not failing in lateral torsional buckling) have the same strength prediction via the AISI Specification. This is inadequate – until L_b exceeds L_{cr} the distortional buckling stress and the strength will decrease.

An integrated design method that employs local and distortional buckling calculations are possible and reliable. The systematic error for large h/b observed in the AISI Specification is alleviated in either of the proposed methods (M_1 or M_2). The test to

predicted ratio is slightly on the conservative side (>1) for the overall results of the proposed models. The standard deviation and number of unconservative predictions are both lower than the AISI Specification for the overall results.

Often, including the local buckling interaction (M_2) actually yields a more conservative prediction than that determined by ignoring it and using an element approach (M_1). However, individual cases are observed where including the local buckling interaction yields markedly better results. Local buckling initiated by long lips and local buckling with highly slender webs and compact flanges are examples where including the interaction is observed to improve the strength prediction markedly.

CONCLUSIONS

Laterally braced cold-formed steel flexural members with edge stiffened flanges have two important buckling phenomena: local and distortional. Current AISI Specification methods do not explicitly treat the distortional mode. Distortional buckling deserves special attention because it has the ability to control the final failure mechanism in many cases and is observed to have lower post-buckling capacity than local buckling. New hand methods are developed to predict the critical buckling stress in both the local and distortional mode. A design method for strength prediction, based on the unified effective width approach, is developed. The design method uses the new expressions for prediction of the local and distortional buckling stress and also introduces a new approach for determining the effective width of the web. The resulting design method is compared to a large body of experimental results and shown to provide more consistent and conservative prediction than the existing AISI Specification. Proper incorporation of the distortional buckling phenomena is imperative for accurate strength prediction of cold-formed steel members.

ACKNOWLEDGEMENT

The sponsorship of the American Iron and Steel Institute in conducting this research is gratefully acknowledged.

APPENDIX I. REFERENCES

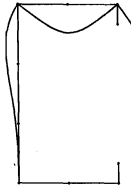
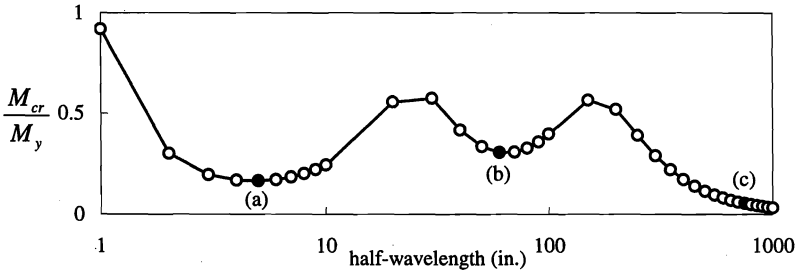
- American Iron and Steel Institute (1996). AISI Specification for the Design of Cold-Formed Steel Structural Members. *American Iron and Steel Institute*. Washington, D.C.
- Cheung, Y.K. (1976). *Finite Strip Method in Structural Analysis*. Pergamon Press, New York.
- Cohen, J. M. (1987). Local Buckling Behavior of Plate Elements, *Department of Structural Engineering Report*, Cornell University, Ithaca, New York.
- Davies, J.M., Jiang, C. (1996). "Design of Thin-Walled Beams for Distortional Buckling." *Proceedings of the Thirteenth International Specialty Conference on Cold-Formed Steel Structures*, St. Louis, Missouri.
- Desmond T.P., Peköz, T. and Winter, G. (1981a). "Edge Stiffeners for Thin-Walled Members." *Journal of the Structural Division*, ASCE, February 1981.
- Elhouar, S., Murray, T.M. (1985) "Adequacy of Proposed AISI Effective Width Specification Provisions for Z- and C-Purlin Design." *Fears Structural Engineering Laboratory*, FSEL/MBMA 85-04, University of Oklahoma, Norman, Oklahoma.
- Ellifritt, D. Spoto, T., Haynes, J. (1992). "Flexural Capacity of Discretely Braced C's and Z's." *Proceedings of the Eleventh International Specialty Conference on Cold-Formed Steel Structures*, St. Louis, Missouri.

- Ellifritt, D., Glover, B., Hren, J. (1997) "Distortional Buckling of Channels and Zees Not Attached to Sheathing." Report for the American Iron and Steel Institute.
- Hancock, G.J. (1995). "Design for Distortional Buckling of Flexural Members." *Proceedings of the Third International Conference on Steel and Aluminum Structures*, Istanbul, Turkey.
- Hancock, G.J. (1997). "Design for Distortional Buckling of Flexural Members." *Thin-Walled Structures*, 27(1).
- Hancock, G.J., Kwon, Y.B., Bernard, E.S. (1994) "Strength Design Curves for Thin-Walled Sections Undergoing Distortional Buckling." *Journal of Constructional Steel Research*, 31(2-3), 169-186.
- Hancock, G.J., Rogers, C.A., Schuster, R.M. (1996). "Comparison of the Distortional Buckling Method for Flexural Members with Tests." *Proceedings of the Thirteenth International Specialty Conference on Cold-Formed Steel Structures*, St. Louis, MO.
- HKS. (1995) ABAQUS Version 5.5. *Hibbitt, Karlsson & Sorensen, Inc.* Pawtucket, RI.
- LaBoube, R.A., Yu, W. (1978). "Structural Behavior of Beam Webs Subjected to Bending Stress." *Civil Engineering Study Structural Series*, 78-1, Department of Civil Engineering, University of Missouri-Rolla, Rolla, Missouri.
- Lau, S.C.W. (1988). Distortional Buckling of Thin-Walled Columns. Ph.D. Thesis, University of Sydney, Sydney, Australia.
- Lau, S.C.W., Hancock, G.J. (1987). "Distortional Buckling Formulas for Channel Columns", *ASCE Journal of Structural Engineering*, 113(5).
- Moreyra, M.E. (1993). The Behavior of Cold-Formed Lipped Channels under Bending. M.S. Thesis, Cornell University, Ithaca, New York.
- Peköz, T. (1987). *Development of a Unified Approach to the Design of Cold-Formed Steel Members*. American Iron and Steel Institute Research Report CF 87-1.
- Rogers, C.A., Schuster, R.M. (1995) "Interaction Buckling of Flange, Edge Stiffener and Web of C-Sections in Bending." *Research Into Cold Formed Steel, Final Report of CSSBI/IRAP Project*, Department of Civil Engineering, University of Waterloo, Waterloo, Ontario.
- Schafer, B.W., Peköz, T.P. (1998). "Computational Modeling of Cold-Formed Steel: Characterizing Geometric Imperfections and Residual Stresses." *Journal of Constructional Steel Research*. (Accepted for Publication)
- Schardt, R. Schrade, W. (1982). "Kaltprofil-Pfetten." Institut Für Statik, Technische Hochschule Darmstadt, Bericht Nr. 1, Darmstadt.
- Schuster, R.M. (1992). "Testing of Perforated C-Stud Sections in Bending." Report for the Canadian Sheet Steel Building Institute, University of Waterloo, Waterloo Ontario.
- Seah, L.K., Rhodes, J. (1993). "Simplified Buckling Analysis of Plate with Compound Edge Stiffeners." *ASCE Journal of Engineering Mechanics*, 119(1), 19-38.
- Shan, M., LaBoube, R.A., Yu, W. (1994). "Behavior of Web Elements with Openings Subjected to Bending, Shear and the Combination of Bending and Shear." *Civil Engineering Study Structural Series*, 94-2, Department of Civil Engineering, University of Missouri-Rolla, Rolla, Missouri.
- Sharp, M.L. (1966). "Longitudinal Stiffeners for Compression Members." *Journal of the Structural Division*, ASCE, October 1966.
- von Kármán, T., Sechler, E.E., Donnell, L.H. (1932). "The Strength of Thin Plates In Compression." *Transactions of the ASME*, 54, 53-57.
- Willis, C.T., Wallace, B. (1990). "Behavior of Cold-Formed Steel Purlins under Gravity Loading." *Journal of Structural Engineering*, ASCE. 116(8).
- Winter, G., (1947) "Strength of Thin Steel Compression Flanges." *Transactions of ASCE*, Paper No. 2305, Trans., 112, 1.

APPENDIX II. NOTATION

b	= flange width	$k_{\phi wg}$	= geometric rotational stiffness of the web
b_e	= effective flange width	k_{xf}	= flange model spring stiffness in x direction
D	= plate rigidity	k_{yf}	= flange model spring stiffness in y direction

f	= stress	$\tilde{k}_{\phi g}$	= $k_{\phi g} / f$
f_1	= edge stress on an element	L	= length
f_2	= edge stress on an element	L_b	= unbraced length
f_{cr}	= minimum buckling stress	L_{cr}	= length at which f is a minimum
f_u	= ultimate failure stress for a member	M	= moment
f_y	= material yield stress	\underline{M}	= consistent nodal moment
h	= web height	M_1	= moment capacity by proposed method 1
h_1	= portion of effective width of a web	M_2	= moment capacity by proposed method 2
h_2	= portion of effective width of a web	M_{AISI}	= moment capacity by the AISI Specification
k	= plate buckling coefficient	R_d	= reduction factor for distortional buckling stress
k_{ϕ}	= rotational stiffness at the web/flange juncture	t	= thickness
$k_{\phi fe}$	= elastic rotational stiffness of the flange	u	= flange model displacement in x
$k_{\phi fs}$	= geometric rotational stiffness of the flange	v	= flange model displacement in y
$k_{\phi we}$	= elastic rotational stiffness of the web	ξ	= stress gradient
ρ	= post-buckling reduction factor	ϕ	= flange model twist
θ	= orientation angle of the edge stiffener (lip)	λ	= slenderness



(a) Local Buckling



(b) Distortional Buckling



(c) Lateral-Torsional Buckling

Figure 1. Finite Strip Analysis of a Flexural Member with an Edge Stiffened Flange

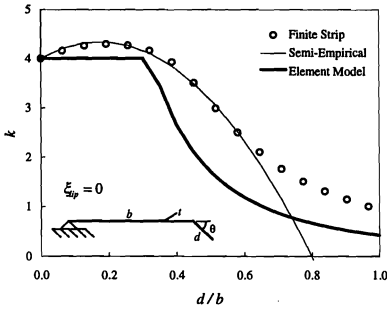


Figure 2. Local Buckling of Isolated Flange and Lip

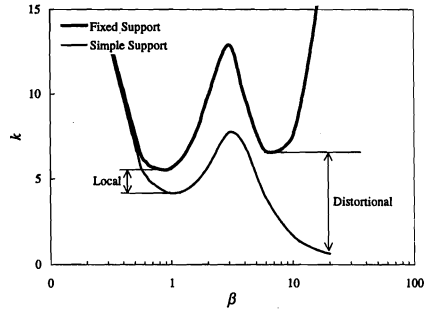


Figure 3. Finite Strip Analysis of Isolated Flange and Lip

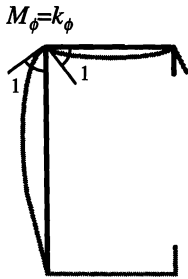


Figure 4. Rotational Stiffness at Web/Flange Junction

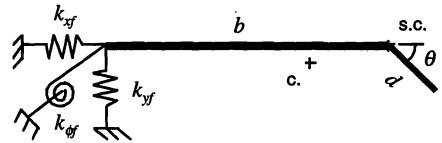


Figure 5. Flange Model

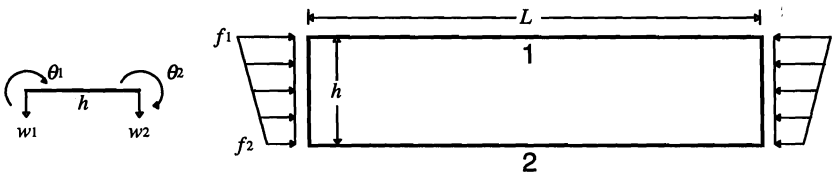
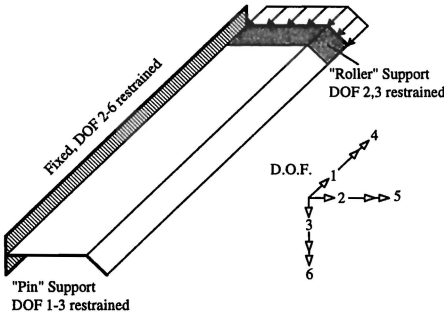
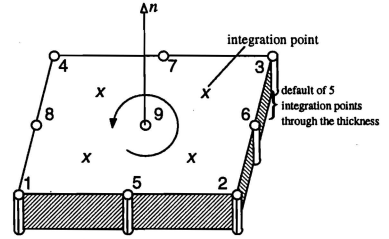


Figure 6. Finite Strip Idealization of the Web

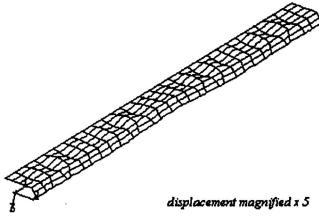


(a) Boundary Conditions and Loading

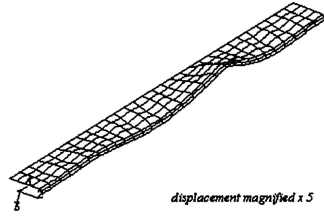


(b) Abaqus S9R5 Shell Element

Figure 7. Finite Element Analysis of Edge Stiffened Flanges



(a) Local Failure



(b) Distortional Failure

Figure 8. Displaced Shape at Peak Load for Edge Stiffened Flanges

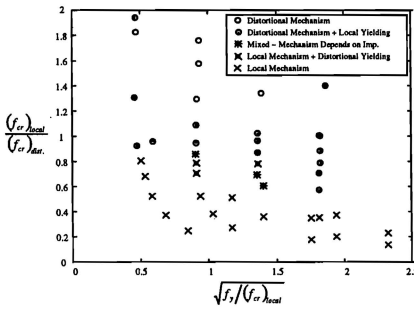


Figure 9. Failure Mode of Edge Stiffened Flanges

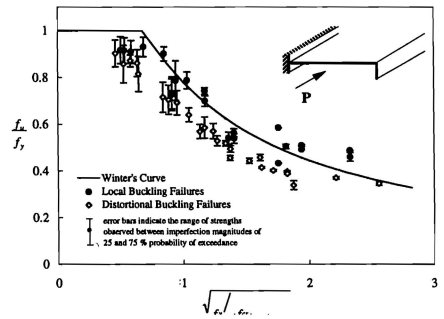


Figure 10. Post-Buckling Capacity of Edge Stiffened Flanges

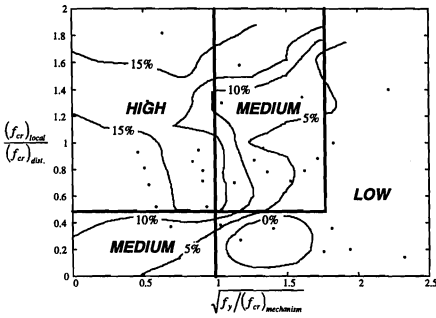


Figure 11. Imperfection Sensitivity of Edge Stiffened Flanges

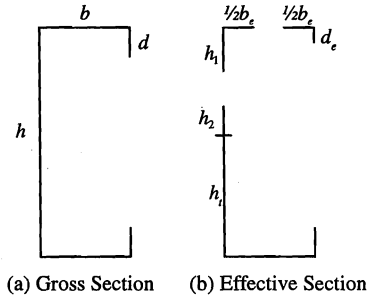


Figure 12. Typical Gross and Effective Section

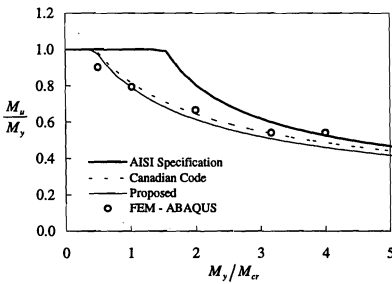


Figure 13. Simply Supported Plate in Pure Bending

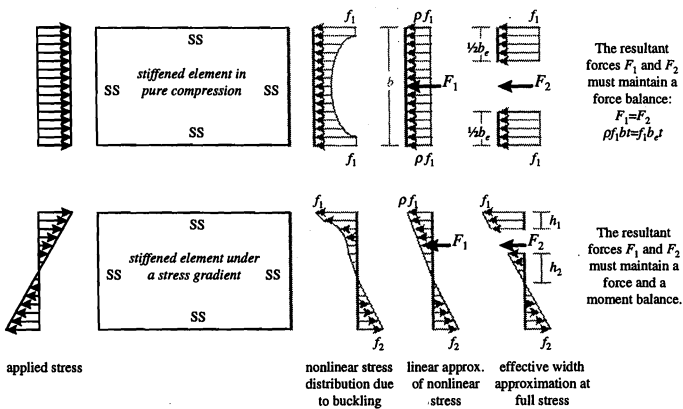


Figure 14. Effective Width Determination

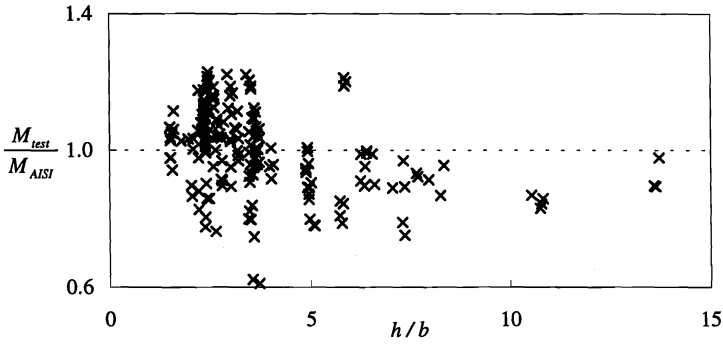
Figure 15. Performance of AISI Specification vs. h/b

Table 1. Local Plate Buckling Coefficients

ELEMENT MODEL

Flange: $(f_{cr})_f \quad k = 4$

Web: $(f_{cr})_w \quad k = (0.5\xi_{web}^3 + 4\xi_{web}^2 + 4)(b/h)^2$

Lip: $(f_{cr})_l \quad k = k_{lip}(b/d)^2$

for $0 < \xi_{lip} \leq 1.1 \quad k_{lip} = 1.4\xi_{lip}^2 - 0.25\xi_{lip} + 0.425$

for $1.1 < \xi_{lip} \leq 2 \quad k_{lip} = 13\xi_{lip}^3 - 65.5\xi_{lip}^2 + 131\xi_{lip} - 80$

SEMI-EMPIRICAL INTERACTION MODEL

Flange/Lip: $(f_{cr})_{fl} \quad k = (8.55\xi_{lip} - 11.07)(d/b)^2 + (-1.59\xi_{lip} + 3.95)(d/b) + 4$
for $\xi_{lip} \leq 1$ and $d/b \leq 0.6$

Flange/Web: $(f_{cr})_{fw} \quad k = 1.125 \min \left\{ 4, (0.5\xi_{web}^3 + 4\xi_{web}^2 + 4)(b/h)^2 \right\}$

Table 2. Geometry of Members

h	b	d	θ
50	25	6.25,12.5	45,90
100	25	6.25,12.5	45,90
	50	6.25,12.5,25	45,90
150	25	6.25,12.5	45,90
	50	6.25,12.5,25	45,90
	75	6.25,12.5,25,37.5	45,90
200	25	6.25,12.5	45,90
	50	6.25,12.5,25	45,90
	75	6.25,12.5,25,37.5	45,90
	100	6.25,12.5,25,37.5,50	45,90

Table 3. Performance of Elastic Buckling Methods

	Local Buckling		Distortional Buckling
	Element Model $M_{predicted}/M_{local}$	Interaction Model $M_{predicted}/M_{local}$	Proposed Method $M_{predicted}/M_{dist.}$
Average	0.74	0.90	0.95
St. Dev.	0.12	0.05	0.08

Table 4. Geometry of Edge Stiffened Flanges

b/t	d/t	θ	$P_{cr,local}$
			$P_{cr,dist}$
25	4.00 - 19.0	90	1.82 - 0.25
	6.25 - 12.5	45	1.94 - 0.96
50	5.00 - 25.0	90	1.58 - 0.27
	6.25 - 25.0	45	1.76 - 0.51
75	6.25 - 37.5	90	1.34 - 0.18
	6.25 - 37.5	45	1.73 - 0.35
100	6.25 - 50.0	90	1.40 - 0.14
	6.25 - 50.0	45	1.75 - 0.23

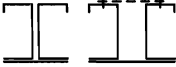
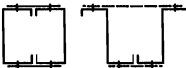
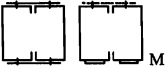
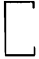
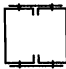

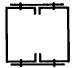
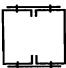

Table 5. Example for Effective Section Calculation

Element	A	y	Ay	Ay ²	I _{own}
C. Flange	$b_e t$	-	-	-	-
Web 1	$h_1 t$	$h_1/2$	$(h_1)^2 t/2$	$(h_1)^3 t/4$	$t(h_1)^3/12$
Web 2	$h_2 t$	$h - (h_1 + h_2/2)$
Web 3	$h_3 t$	$h - (h_1/2)$
T. Flange	bt	h
C. Lip	$d_e t$	$d_e/2$
T. Lip	dt	$h - d/2$
$\sum A$			$\sum Ay$	$\sum Ay^2$	$\sum I_{own}$
$M_n = S_{eff} f_1 \quad S_{eff} = \frac{I_{eff}}{y_{eff}} \quad y_{eff} = \frac{\sum Ay}{\sum A} \quad I_{eff} = \sum Ay^2 + \sum I_{own} - (\sum A)y_{eff}^2$					

Table 6. Elastic Buckling Stress Determination

Model 1 ~ M_1	Model 2 ~ M_2
No Local Buckling Interaction	Local Interaction Included
$(f_{cr})_{web} = \min[(f_{cr})_w, R_d(f_{cr})_d]$	$(f_{cr})_{web} = \min[(f_{cr})_{fw}, R_d(f_{cr})_d]$
$(f_{cr})_{flange} = \min[(f_{cr})_f, R_d(f_{cr})_d]$	$(f_{cr})_{flange} = \min[(f_{cr})_{fw}, (f_{cr})_{fl}, R_d(f_{cr})_d]$
$(f_{cr})_{lip} = \min[(f_{cr})_l, R_d(f_{cr})_d]$	$(f_{cr})_{lip} = \min[(f_{cr})_{fl}, R_d(f_{cr})_d]$

Table 7. Summary of Test to Predicted Ratios

Researcher and the basic geometry/setup					$\frac{M_{test}}{M_{AISI}}$	$\frac{M_{test}}{M_1}$	$\frac{M_{test}}{M_2}$
		max	min				
Cohen (1987) 	h/t	128	78	Avg.	1.08	1.02	1.02
	b/t	55	33	St. Dev.	0.05	0.11	0.11
	d/t	16	9	min	0.99	0.93	0.92
	$\sqrt{f_y/f_w}$	1.3	0.4	n<1 of 18	2	6	5
Ellifritt et al. (1997) 	h/t	139	113	Avg.	0.78	0.91	0.91
	b/t	48	31	St. Dev.	0.10	0.11	0.11
	d/t	16	11	min	0.61	0.75	0.75
	$\sqrt{f_y/f_w}$	1.5	1.2	n<1 of 10	10	8	8
Laboube and Yu (1978) 	h/t	269	77	Avg.	1.02	1.07	1.11
	b/t	75	28	St. Dev.	0.08	0.08	0.10
	d/t	15	11	min	0.87	0.88	0.92
	$\sqrt{f_y/f_w}$	1.2	0.7	n<1 of 32	11	7	6
Moreyra (1993) 	h/t	124	120	Avg.	0.86	0.96	0.99
	b/t	36	34	St. Dev.	0.08	0.11	0.09
	d/t	16	12	min	0.80	0.86	0.91
	$\sqrt{f_y/f_w}$	1.0	0.6	n<1 of 6	5	5	5
Rogers (1995) 	h/t	228	53	Avg.	1.02	1.09	1.11
	b/t	61	15	St. Dev.	0.11	0.07	0.07
	d/t	34	3	min	0.83	0.94	0.94
	$\sqrt{f_y/f_w}$	1.8	0.5	n<1 of 49	26	6	2
Schardt and Schrade (1982) 	h/t	183	178	Avg.	1.05	1.05	1.09
	b/t	71	45	St. Dev.	0.10	0.09	0.08
	d/t	16	10	min	0.89	0.92	0.96
	$\sqrt{f_y/f_w}$	1.4	0.6	n<1 of 37	14	13	7
Schuster (1992) 	h/t	168	166	Avg.	0.82	0.97	1.01
	b/t	34	33	St. Dev.	0.04	0.05	0.05
	d/t	11	10	min	0.78	0.93	0.97
	$\sqrt{f_y/f_w}$	1.0	1.0	n<1 of 5	5	3	3
Shan et al. (1994) 	h/t	256	43	Avg.	0.97	0.97	1.04
	b/t	58	19	St. Dev.	0.13	0.10	0.09
	d/t	20	6	min	0.75	0.79	0.85
	$\sqrt{f_y/f_w}$	1.0	0.4	n<1 of 29	18	22	10
Willis and Wallace (1990) 	h/t	131	126	Avg.	1.02	1.02	1.08
	b/t	40	38	St. Dev.	0.08	0.07	0.08
	d/t	17	14	min	0.92	0.93	0.98
	$\sqrt{f_y/f_w}$	0.7	0.6	n<1 of 4	2	1	1
All Experimental Data	h/t	269	43	Avg.	1.00	1.04	1.07
	b/t	75	15	St. Dev.	0.10	0.08	0.08
	d/t	34	3	min	0.61	0.75	0.75
	$\sqrt{f_y/f_w}$	1.8	0.4	n<1 of 190	93	71	47